Acoustic Design of Elliptical Bells for Chime Sound Simulation

Leyu Zhang *
Shanghai World Foreign Language Academy, Shanghai, China
* Corresponding Author Email: kytbz2023@163.com

Abstract. This project seeks to unravel the opulent acoustical characteristics and sonic effects of ancient Chinese chime bells. Initially, distinctive features of the chime bells are encapsulated, highlighting the bifonic phenomenon and elucidating the role of fundamental and harmonic frequencies in chime bell sound production, while emphasizing the timbral diversity attributable to its multifrequency sound source. An exploration into the impacts of various factors on chime bell sound, such striking position, is conducted through experimentation with a bronze chime bell model, underscoring their significant influence. Employing experimental modal analysis methods, vibrational modes of the chime bell surface at disparate frequencies are revealed, laying a foundation for understanding the sound production principles. Furthermore, image processing technologies are utilized to construct a 3D model of the chime bell, and finite element modal analysis methods are applied to visualize its modes. The feasibility of using a circular ring to simulate chime bell sound is explored, identifying the elliptical ring as a more promising option and undergoing numerous rounds of iterative optimization. The theoretical research is brought to fruition by manufacturing a cast iron elliptical ring model for striking experiments, thereby validating the theoretical insights. In summation, this research provides a comprehensive and systematic exploration into the acoustical mechanisms and design principles of chime bells, offering invaluable insights into ancient Chinese music and cultural heritage. The multi-faceted and rich nature of chime bells as musical instruments is unveiled through the integrated application of various methods, deepening the understanding of their acoustical characteristics.

Keywords: Modal Analysis, Finite Element Analysis, Optimization Design, Bronze Chime Bells, Elliptical Ring.

1. Introduction

Chinese chime bells are an important musical instrument in ancient China, whose origin can be traced back to the Zhou Dynasty. During the Warring States periods, Chinese chime bells were widely used in ceremonial music. The chimes are made of bronze bells of different sizes, which are hung on a huge bell frame in the order of pitch. By hitting each bell with a wooden hammer or a bamboo stick, a different piece of music could be played. Each of the bronze bells in the chime has its own unique pitch. The Zenghouyi Chimes are the largest and most complete set of chimes ever discovered, with 63 pieces of bronze bells and a pitch range spanning two octaves, and have been called the "Eighth Wonder of the Ancient World". The chimes not only represent the achievements in the pentatonic system and the law of sound, but also reflect the high level of bronze casting technology in ancient China. The emergence and development of chimes proves that the Chinese pre-Qin period had successfully solved the problems related to the sound and rhythm of bronze bells.

Pervasive investigations into the acoustic characteristics of ancient Chinese chime bells have been undertaken, with diverse studies illuminating various aspects of their construction and sound production. Profound examinations into the acoustic features of ancient chime bells have unfolded through various dimensions of research and methodology. Focused inquiries by various scholars have illuminated the extensive and nuanced acoustical properties of these historical instruments. Wang [1] explored its acoustical characteristics through spectral and time-frequency analyses, particularly emphasizing pitch, timbre, and sound decay effects, while also indicating pitch variations and ranges amongst different chime bell sets. Han [2] addressed the formulation of musical scales from an acoustics perspective, explicating the intertwined relationship between musical scales and the acoustic structure of chime bells, with a spotlight on aiding tuning through orchestral sound production devices, thereby associating bell tuning with string instrument tuning. Pan [3], utilizing physical methods to measure bell frequencies, discovered that this set of chime bells spans three octaves, with scales approximating pure temperament, and all being flat-mouthed, dual-tone bells. Differently, Jia [4] and Zhang [5] embarked from a vibration mode standpoint, with the former employing electromagnetic exciters and laser holography, and the latter finite element analysis, both profoundly exploring the vibrational characteristics and sound production mechanisms of chime bells.

In the in-depth research into physical and acoustical characteristics, Yan [6] utilized a cylindrical model, amalgamating elastic standing wave theory and the rigidity characteristics of an elliptical column surface, to analyze the acoustic features of ancient chime bells. Xu [7] delved into the relationship between the shape and sound-producing characteristics of bronze bells from a vibrational theory perspective, especially underscoring key tuning methods in bell casting.

Despite extensive literature review, it has been discerned that the musical theories and playing methodologies of ancient chime bells remain partially enigmatic, with no extant sheet music or sound recording [8]. Due to the passage of time, the original production process of chime bells has been gradually lost, and most of the surviving ones are the products of restoration by later generations of artists. In order to gradually restore the production process of the chimes and to reproduce the technique and sound of the chime bells, an oval shape modal is constructed to propel further exploration into the acoustics of chime bells within this research.

The primary objective herein is to investigate the sound characteristics of ancient Chinese bronze chime bells, scrutinizing the acoustic principles behind the "dual tones per bell" phenomenon [9]. A secondary aim entails designing a chime bell embodying "dual tones per bell" features, comparing its timbre and pitch with traditional bronze chime bells to validate the design model.

This research unfolds through structured Sections: Section 2 encapsulates the characteristics of bronze chime bells, highlighting the dual-tone phenomenon and delineating the role of fundamental and harmonic frequencies in sound production. Section 3 investigates the chime bell surface’s vibration modes at different frequencies utilizing experimental modal analysis methods. Section 4 employs image processing technology to construct a three-dimensional model of the chime bell and applies finite element modal analysis for visualizing its vibration characteristics. Section 5 and 6 iteratively designs the elliptical ring, conducting striking experiments using a cast-iron elliptical ring model and detailing pivotal steps and conclusions of the design. Conclusively, Section 6 synthesizes the paper's entirety, identifies research shortcomings, and suggests potential trajectories for subsequent experiments.

2. Methodology and Preliminary Observations on the Sound Characteristics of Bronze Chime Bells

This section focuses on the methodology and preliminary observations regarding the sound characteristics of bronze chime bells by utilizing a miniature model of the bronze chime bell and employing a meticulous approach for sound analysis.

The rich resonant characteristics of bronze chime bells, celebrated throughout history, served as a foundation for this in-depth experimental study. This research utilized a miniature model of the bronze chime bell (see Figure.1), weighing approximately 250 grams, aiming to explore its sound attributes under varied striking conditions.

Figure 1. Model of Bronze Chime Bell

A meticulous approach was taken to ensure rigorous sound analysis. As shown in Figure. 2, the experimental setup incorporated the Chengke Dynamic Force Sensor CT-LC-01. When complemented with an impact hammer, this sensor allows for various hammerhead adjustments, optimizing contact time. Four microphones were strategically positioned around the bell to achieve comprehensive sound capture.

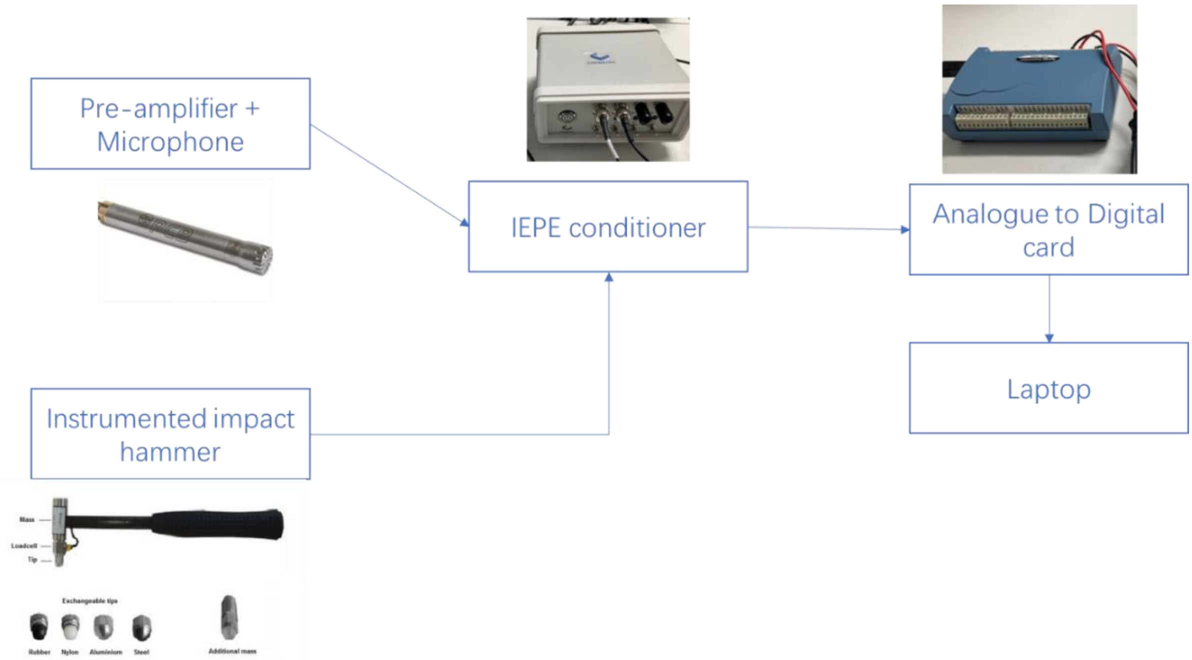

Figure 2. schematic sketch of data acquisition system

Recognizing the crucial role of striking strength in sound generation, a consistent methodology was enforced to control the bell's excitation, emphasizing uniform force and speed at designated strike points. The experiments highlighted the inherent directionality of the bell's sound, which remains evident even with consistent strikes at a single location. Variations in sound propagation, as portrayed in Figure 3, shed light on the impact of microphone positioning. Furthermore, frequency response functions pinpointed specific strike locations more likely to produce distinct tonalities.

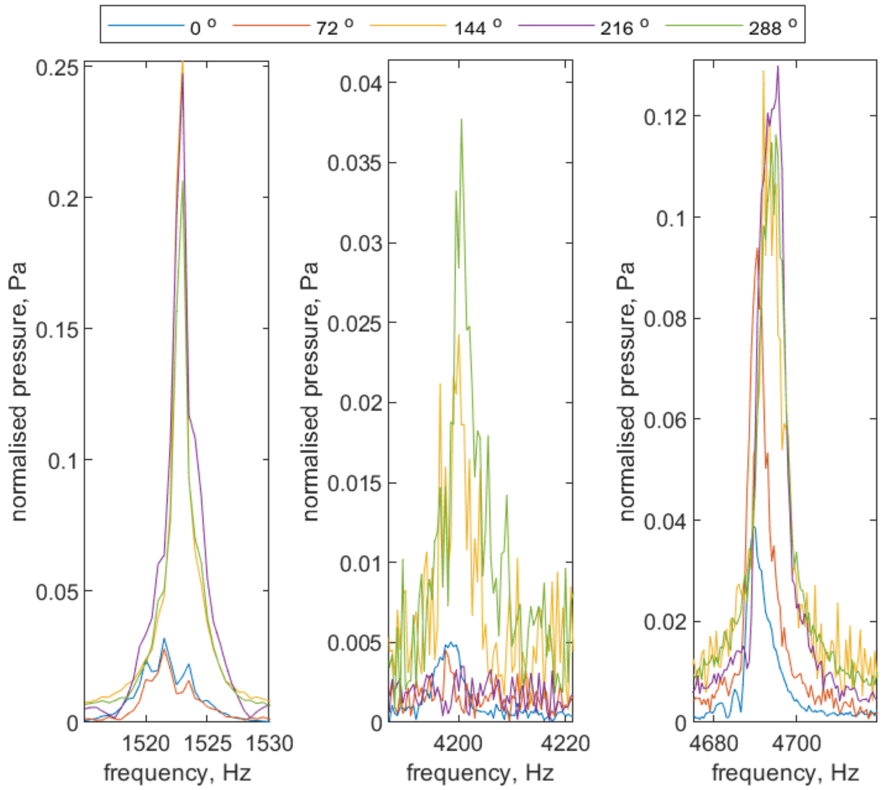

Figure 3. Normalized Sound Pressure for the Microphones at Different Locations Around the Bell

A comparative analysis between direct and side strikes revealed different resonance mode activations (see Figure 4). As an illustration, a direct 0° strike prominently resonated the 1523 Hz and 4692 Hz modes, whereas a 45° strike induced the 4200 Hz and 4692 Hz modes.

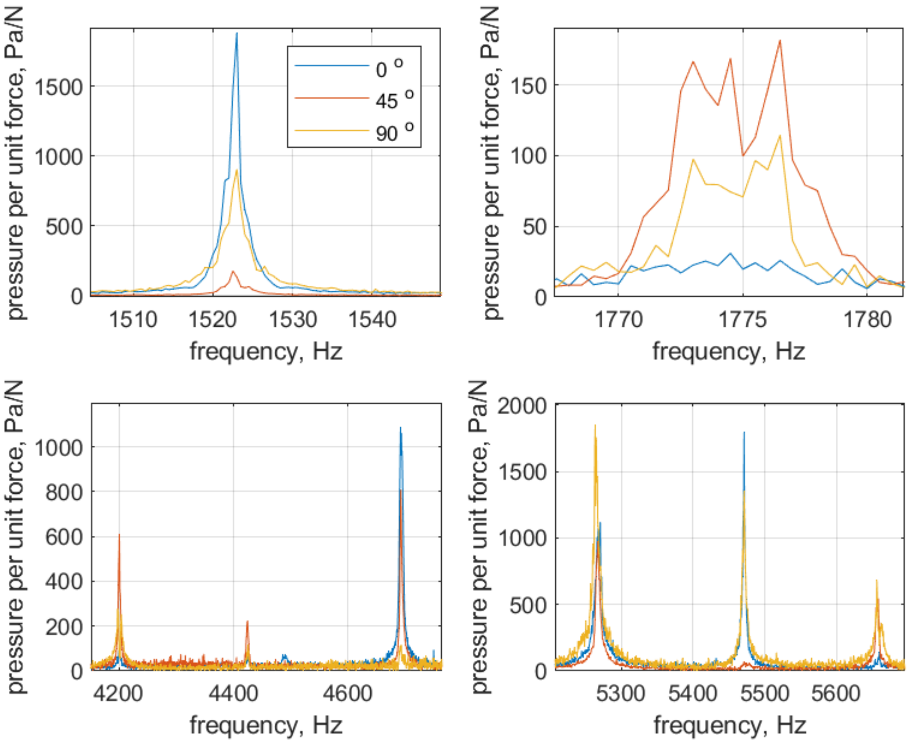

Figure 4. normalized sound pressure when subject to different excitation locations

The focused experiments elucidate the nuanced influence of strike method and location on the resonance and tonal qualities of bronze chime bells. These preliminary insights contribute to a broader understanding of these musical instruments.

3. Experimental Modal Analysis of Chime Bells

In previous section, the intricate relationship between the sound of chime bells and their vibrational modes at varying frequencies was highlighted. These modes, encapsulating the fundamental attributes of the bells, remain independent of excitation sources and data collection points. Different frequencies display distinctive displacements and phases, shedding light on the chime bells' various vibrational modes [24]. This detailed study facilitates deeper comprehension of the sound production mechanisms of the bells.

Physical structures, based on their inherent characteristics like mass, stiffness, and damping, resonate at specific frequencies. These resonances, fundamental to modal analysis, dictate how a structure vibrates at different frequencies. In mathematical terms, this behavior can be described using eigenvectors, which represent relative displacements across various points of the structure. Each eigenvector consists of complex numbers that capture both amplitude and phase details of the vibration. The frequency response function, representing the system's response to excitation, can be denoted as:

$$\alpha_{ij} = \frac{\phi_{in}\phi_{out}}{-m\omega^2 + k + jc\omega} \tag{1}$$

In this equation, ϕ_{in} and ϕ_{out} symbolize the physical modal vectors for excitation and vibration collection positions. Other variables, m, k, and c, correspond to modal attributes like mass, stiffness, and damping, respectively, while ω stands for the excitation frequency.

During the chime bells' modal analysis, force sensors and accelerometers act as data collection instruments. The chime bells are struck using force sensors and an impact hammer, while accelerometers gauge the bells' accelerative reactions. These instruments are managed through a signal conditioner, linked to an Analog-to-Digital Converter (ADC) card, which transitions analog signals to digital. A laptop subsequently accumulates time-domain signal data for both acceleration and force. The entire experimental configuration can be seen in Figure 5.

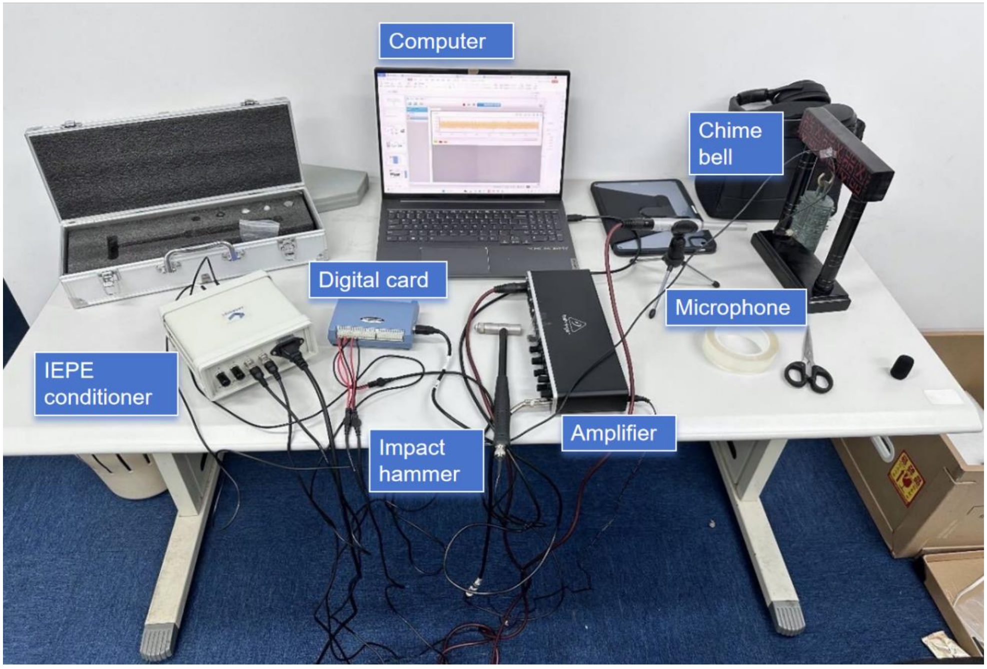

Figure 5. Experimental Apparatus Schematic for Chime Bells Modal Analysis

Upon securing the time-domain signals for acceleration and force, a Fourier transform yields their spectral representations. By determining the acceleration spectrum to force spectrum ratio, the frequency response function at particular points is acquired. This data underpins the investigation into the vibrational characteristics of the chime bells across frequencies.

Given the axial symmetry of the chime bells, twelve uniformly distributed excitation points were selected on a quarter of the bell's surface. These striking points span various locations, with specific attention to the 0-degree front, 30-degree, and 60-degree directions. Figure 6 showcases each point's precise position, with the coordinate system's origin at the chime bell's top center. Numerical designations from 1 to 12 were allocated for each striking point, ensuring precision during experimentation and data interpretation.

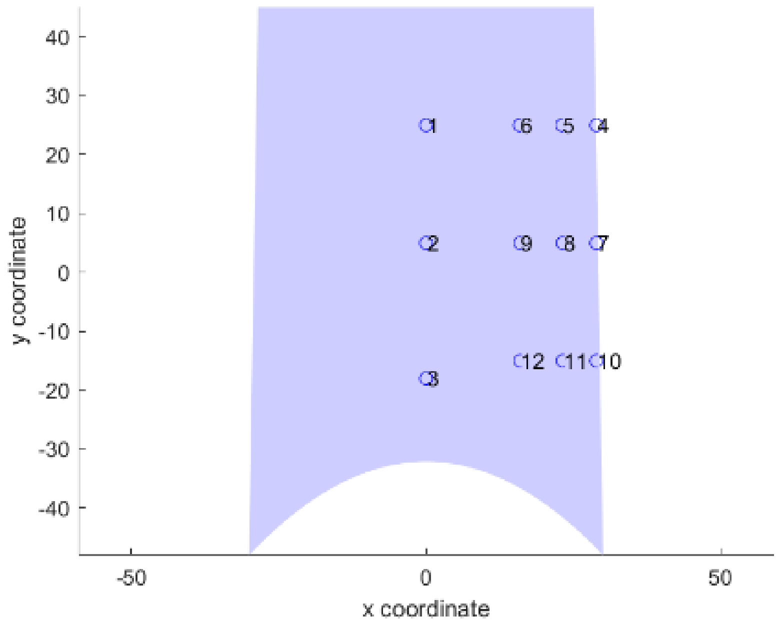

Figure 6. Schematic of Various Vibration Points on Chime Bells

Each striking location experienced ten repeated strikes, undergoing ensemble averaging to curtail noise levels in the frequency response function. Metallic hammerheads, offering a closer simulation of genuine chime bell tonalities, were chosen based on preliminary experiments. These confirmed that the force signal spectrum from the metallic hammerheads supplied adequate excitation energy within the required frequency spectrum, guaranteeing the accuracy of the frequency response function.

The frequency response functions spanning various striking points are depicted in Figure 7. It becomes apparent that, when striking position 1, the modal around 1400 Hz is more readily stimulated than the modal proximate to 1750 Hz.

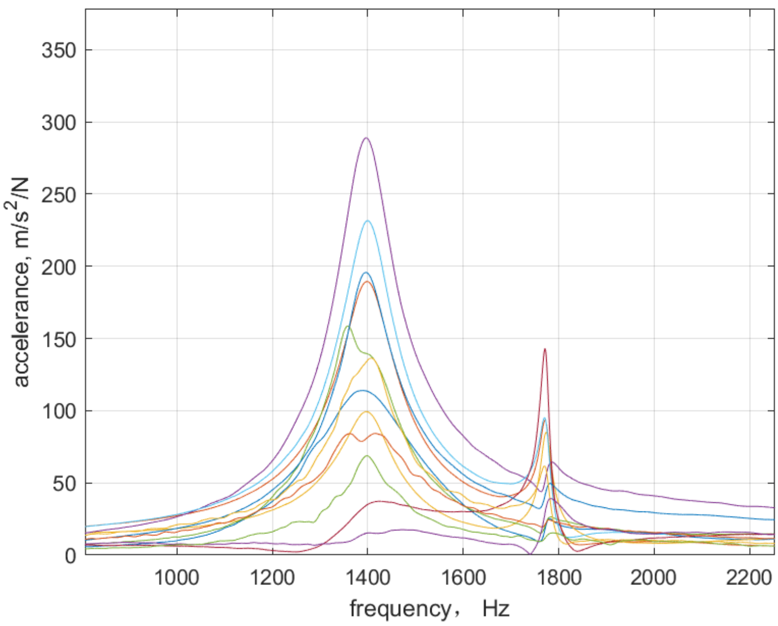

Figure 7. Frequency Response Functions at Different Striking Positions

The mode shape of these two resonances are shown in Figure 8. The 1400 Hz modal displays heightened modal deformations at the upper region of the 0-degree front position. This suggests the bell's strike at the 0-degree location predominantly excites this frequency modal. Conversely, the 1750 Hz modal remains negligible at this strike point, implying suppressed vibrations at 1750 Hz, leading to the predominance of tones circling 1400 Hz.

Observing the 1750 Hz modal, the modal shapes reveal peak modal deformation around the 30-degree mark. This implies a strike at the 30-degree incline more readily stimulates modals proximate to 1750 Hz. Nonetheless, this strike position might also induce 1400 Hz frequencies. However, the amplitude of this modal remains significantly subdued compared to the 1750 Hz modal, ensuring tones around 1750 Hz remain dominant.

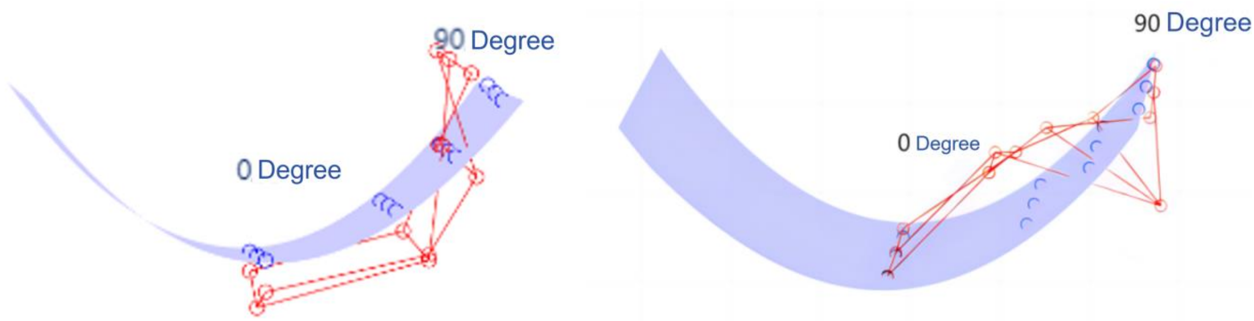

(a) (b)

Figure 8. (a) Identified Modal at 1400 Hz; (b) Identified Modal at 1750 Hz

4. Finite Element Modal Analysis of Chime Bells

In the preceding section, we explored the acoustic characteristics of chime bells and their relationship with structural modes. While experimental modal analysis provides a method to determine the natural frequencies and vibration modes of chime bells, its visualization of vibration modes is not always clear. Thus, this Section employs finite element modal analysis for a more detailed understanding of chime bell vibrational characteristics.

4.1. Geometric Modeling of Chime Bells

Before conducting the finite element analysis, accurate geometric modeling of the chime bell is crucial. For this, we used photography to gather exterior information and then imported it into 3D modeling software. Specifically, a household mobile phone stand and a smartphone were employed to capture images. By taking multiple photographs from various angles with the smartphone's high-resolution camera, we ensured comprehensive coverage of the chime bell's exterior. The raw images were then processed in Photoshop. We isolated the chime bell and set the background to white for clarity. After adjusting and sharpening the images, they were further processed in MATLAB using the Sobel operator for edge detection. Coordinates with black pixels were detected for Solidworks modeling, the images were then used in 3D modeling software, SolidWorks.

4.2. Finite Element Modal Analysis

For the finite element analysis, various finite element cell types were utilized to capture the chime bell’s intricate geometric shapes[11]. The material properties of bronze, the chime bell material, are detailed in Table 1.

Table 1. Physical properties of bronze

Density	8900 kg/m3
Young’s modulus	70 GPa
Poisson’s ratio	0.25

Grid density plays a pivotal role in the accuracy of simulation results. We conducted multiple grid divisions on the chime bell model to assess the finite element model's numerical convergence, as shown in Figure 9.

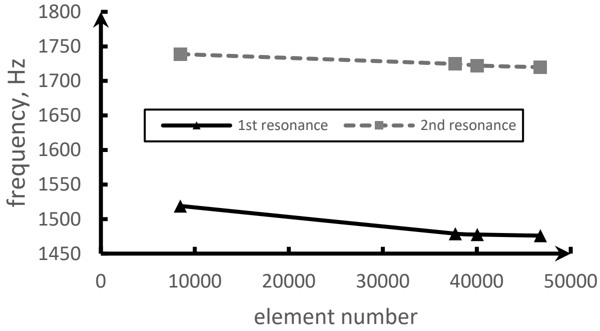

Figure 9. Mesh convergence analysis

With a grid cell size of 1 mm, the results exhibited a stable trend for the first and second-order resonance frequencies. The primary modal vibration forms of the chime bell are depicted in Figure 10.

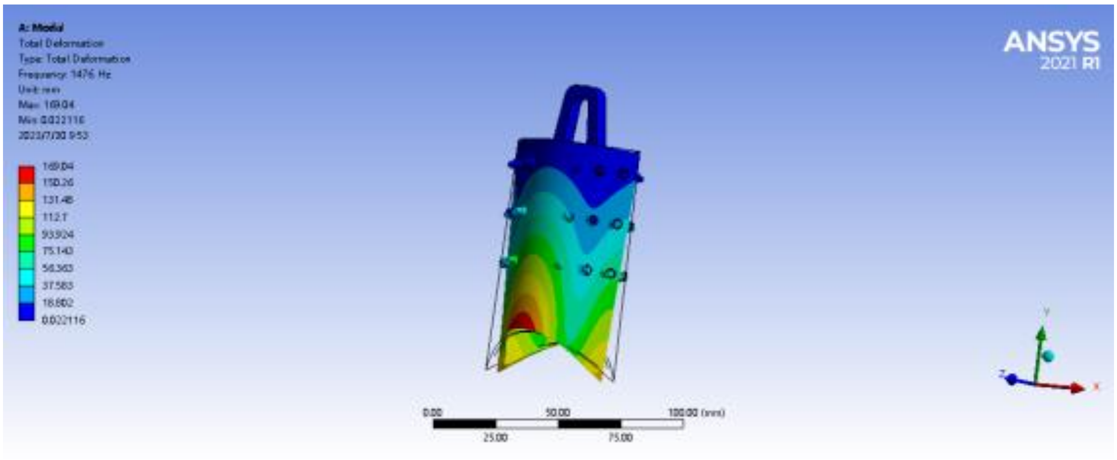

(a)

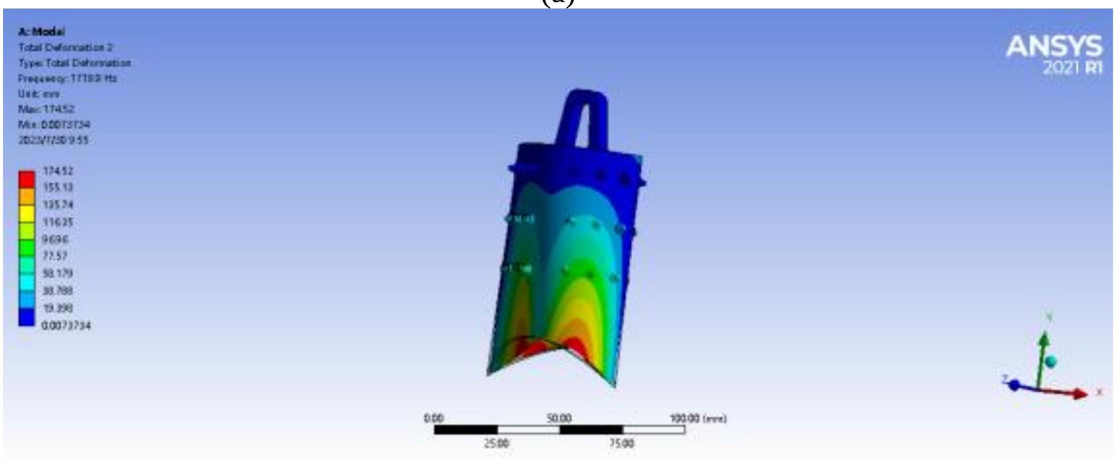

(b)

Figure 10. Typical vibration modes of chime bell (a) Main tone (b) Side tone

Upon comparing the frequencies from the finite element modal analysis with the experimental modal analysis, discrepancies were noted. For the side tone, results aligned closely. However, the main tone showed a divergence of about 80 Hz. Several factors could contribute to this, such as modeling errors or unaccounted details in the chime bell design. The intricacies of the chime bell's design, including protrusions or patterns, could influence its vibrational modes. However, given the accurcy of modelling strategy, capturing these nuances was challenging. The shape of vibrational modes significantly affects the sound's quality and timbre, even if there are minor frequency discrepancies.

Subsequently, the modal consistency criterion is used to gauge the similarity between the finite element modes and those identified experimentally. The modal vectors are listed in Table 2.

Table 2. Modal vectors from experiments and finite element analysis

Location	1st resonance		2nd resonance	
	EXP	FEA	EXP	FEA
u0	-58.9	-17.7	11.9	13.2
m0	-158.3	-53.5	4.3	23.9
b0	-96.4	-84.7	1.7	29.1
u90	62.0	17.8	-4.2	-15.5
u60	5.0	2.1	19.6	13.6
u30	-113.9	-25.5	58.9	14.6
m90	174.2	43.5	-13.4	-7.0
m60	22.8	16.0	-123.7	-46.6
m30	-206.5	-41.0	92.4	55.0
b90	252.7	74.4	-19.9	-19.6
b60	-88.8	-40.5	84.1	75.9
b30	-167.6	-55.2	91.1	102.0

Using the Modal Assurance Criterion, we gauged the similarity between the modal vectors. The resultant values of 0.84 and 0.77 for the first and second modes respectively underscored the reliability of the finite element analysis for chime bell design.

5. Optimization of the elliptical ring bell

In the preceding discussion, the analysis was centred on the bell, examining its characteristics and properties. Challenges arose in achieving two closely adjacent modal frequencies, which prompted exploration into the elliptical ring structure as a potential solution[10]. This section will employ finite element optimization design methods to discern suitable elliptical ring design parameters that can simulate the acoustic performance of the chime bell.

Finite element modal analysis methods will be utilized to study the modal characteristics of elliptical rings, focusing on understanding whether they can support multiple modes within adjacent frequency ranges[12]. The requirement for exactness of the actual modal frequency isn’t particularly stringent. The physical properties of elliptical rings to be used in the simulation are detailed in Table 3.

Table 3. Physical Properties of the Elliptical Ring

Physical quantity	Unit	Value
Major diameter	mm	40
Minor diameter	mm	20
Thickness	mm	2
Height	mm	40
Density	kg/m3	7850
Young’s modulus	GPa	230
Possion’s ratio		0.3

For this finite element model, its mesh characteristics are similar to the finite element mesh types described in the previous section. The results of the finite element modal analysis are shown in Figure 11:

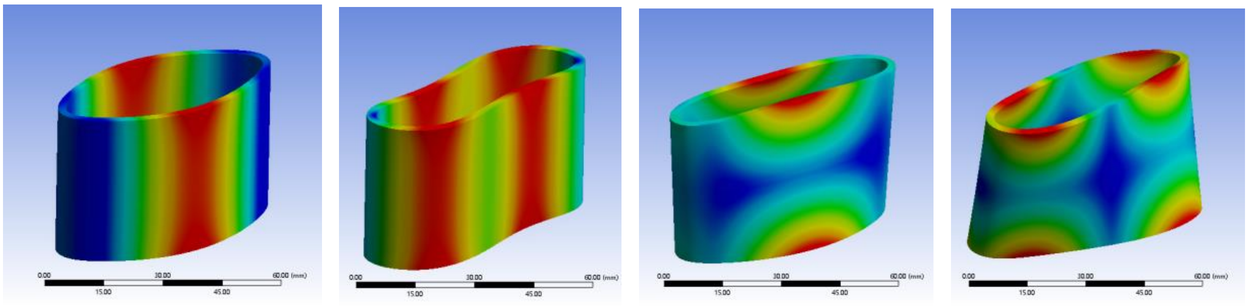

(a)1189 Hz; (b) 1397 Hz; (c) 2043 Hz; (d) 2090 Hz

Figure 11. Results of finite element modal analysis (first four orders)

The insights from Figure 11 suggest that the design of the elliptical ring facilitates the achievement of two different modes within close frequency ranges. These modes, being breathing modes, can conveniently produce effective sound.

The chime bell modes were studied, leading to the successful design optimization of the chime bell model to meet the target frequencies of 1521 and 1722 Hz, utilizing the Ansys platform and Multi-Objective Genetic Algorithm (MOGA). Subsequent to design optimization, design parameters of three chime bell models, closest to the target frequencies, were obtained as detailed in the subsequent table.

Table 4. Results of Elliptical Ring Design Optimization

P1-Minor diameter(m)	P2-Major diameter(m)	P3-Height(m)	P4-Thickness(m)	Resonance frequency for mode 1 (Hz)	Resonance frequency for mode 2 (Hz)
0.03	0.06	0.13948	0.005	1561.1	1815.4

The established model was imported into ANSYS for modal analysis, and the results are displayed in Figure 12 The analysis reveals the presence of four similar modal shapes within the frequency range of 1500 to 2000 Hz.

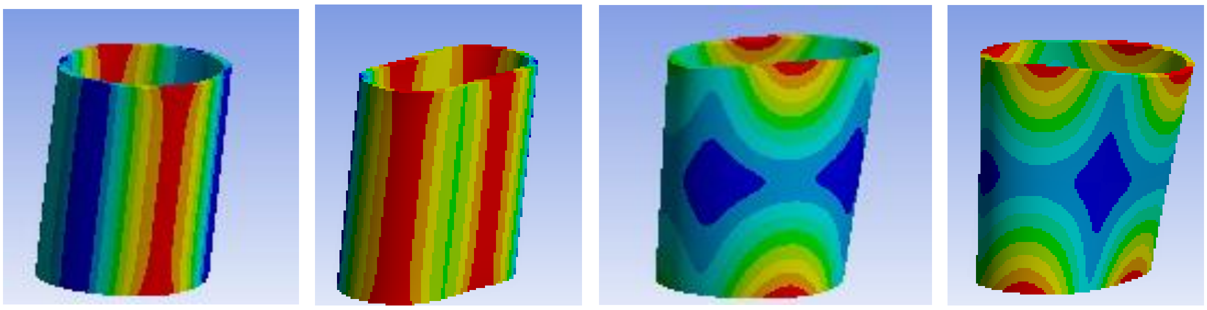

(a) 1561 Hz (b) 1624 Hz (c)1815 Hz (d) 1839 Hz

Figure 12. First four finite element modes of the optimized elliptical ring

To achieve adequate loudness, impact must be applied at the anti-node of the mode. The modal analysis results dictate that to excite the first-order mode without triggering other higher-order modes, impact should be applied at the center height position on the front of the elliptical ring. However, it's vital to note that exciting the first-order mode at this position also strongly excites the second-order mode due to their close proximity, potentially producing auditory noise. Conversely, exciting the second-order mode can be achieved by applying impact at the side center height position of the elliptical ring, where other modes near the nodes are not easily excited. In conclusion, structural adjustments to the current simulation model are necessitated by the results of modal analysis, to more aptly meet the required loudness and sound characteristics.

Drawing inspiration from the pattern structure on bronze chime bells, the structural shape of the elliptical ring was modified by introducing some details, with the aspiration to influence higher-order vibration modes. The goal was to locate positions where specific modes could be excited by applying excitation solely at these points. It was observed that Mode 3 and Mode 4 exhibited significant amplitudes at a 60-degree inclined position on the front face of the chime bell. To suppress the excitation of these two modes, four symmetric vertical bars were added at the 60-degree inclined position on its front face to reduce the mode shape at this position and ultimately make the third and fourth modes harder to excite. These bars matched the chime bell in height and featured a width of 1.5cm and a thickness of 0.3cm. To diminish the overlap of the maximum amplitudes of Mode 1 and Mode 2, a mass block was introduced directly below the chime bell to alter the vibration pattern of Mode 1.

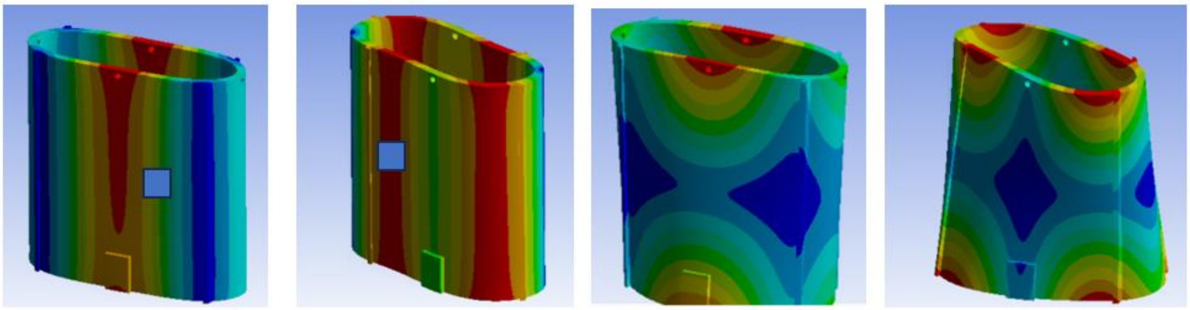

(a) 1st mode (b) 2nd mode (c) 3rd order (d) 4th order

Figure 13. Mode shapes of the elliptical ring with 60-degree vertical bars and bottom bars (the square represents the excitation point)

Ultimately, this optimisation model was selected and cast at a 1:1 ratio.

6. Acoustic Experiment of the Elliptical Ring Bell

In the preceding section, a simple elliptical ring structure was successfully constructed using finite element design methods. This section further verifies this elliptical ring through acoustic experiments to determine whether it can achieve the expected dual-tone sound characteristics and whether its sound frequency aligns with the design expectations. These experiments serve to validate the effectiveness of the utilized design method.

The elliptical ring was fabricated using casting technology, selected primarily for its cost-effectiveness and geometric considerations. Initially, the method involved the cutting of thin steel sheets, followed by gradual bending, and then welding the free ends together. Maintaining the precise roundness of the ellipse during this process proved challenging. Furthermore, the welding operation was quite complicated since both ends of the iron sheet are not on the same plane. Additional welding was required after manufacturing the elliptical ring to finalize various details, making the welding method costly and exceeding the initial budget. Ultimately, casting was chosen, resulting in the cast iron elliptical ring as shown in Figure 14.

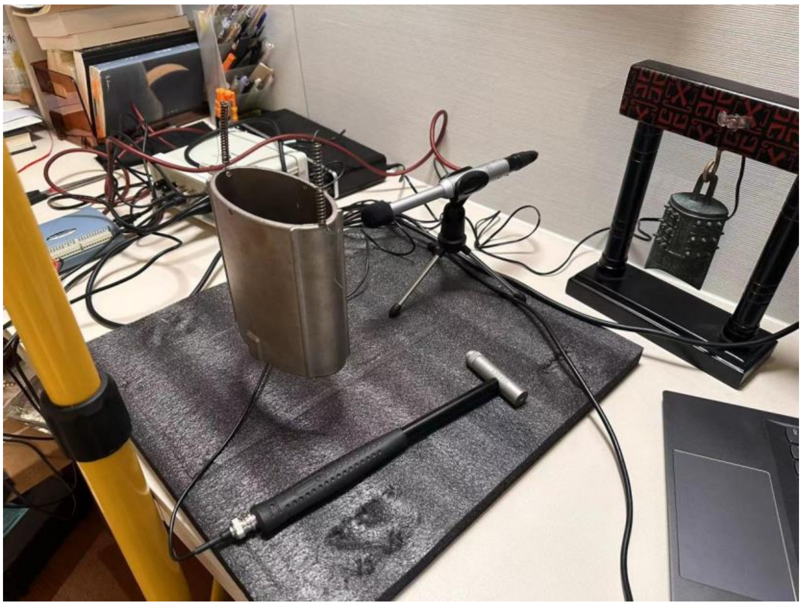

Figure 14. Experimental Equipment for Acoustic Experiment

Microphones were positioned around the elliptical ring at 0h, 2h, 4h, 6h, 8h, and 10h, with 0h corresponding to the major diameter axis of the elliptical ring. Each microphone sampled four strikes at each location, and a frequency domain average was performed to enhance the signal-to-noise ratio. For each experiment set, two fixed locations were always struck; one was dominated by the low tone sound, the other by the high tone sound, as shown in Figure 15.

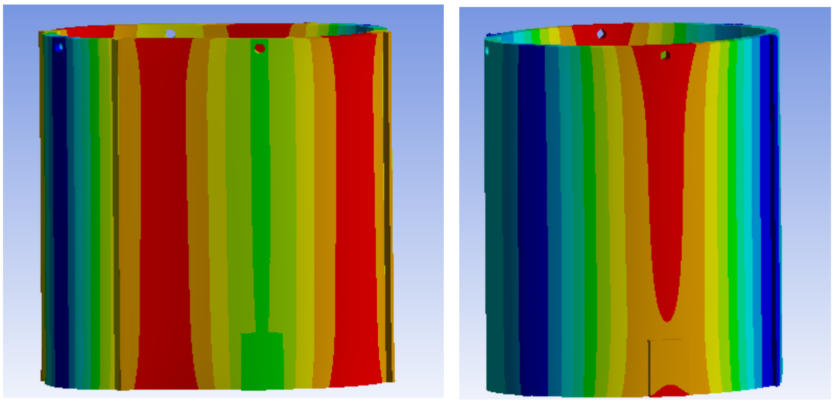

Figure 15. Striking Positions (Red Area) on the Elliptical Ring (Left: Low Tone Sound; Right: High Tone Sound)

The elliptical ring bell was initially struck with a metal hammer, and acoustic signals from five different directions were averaged to study the overall sound characteristics.

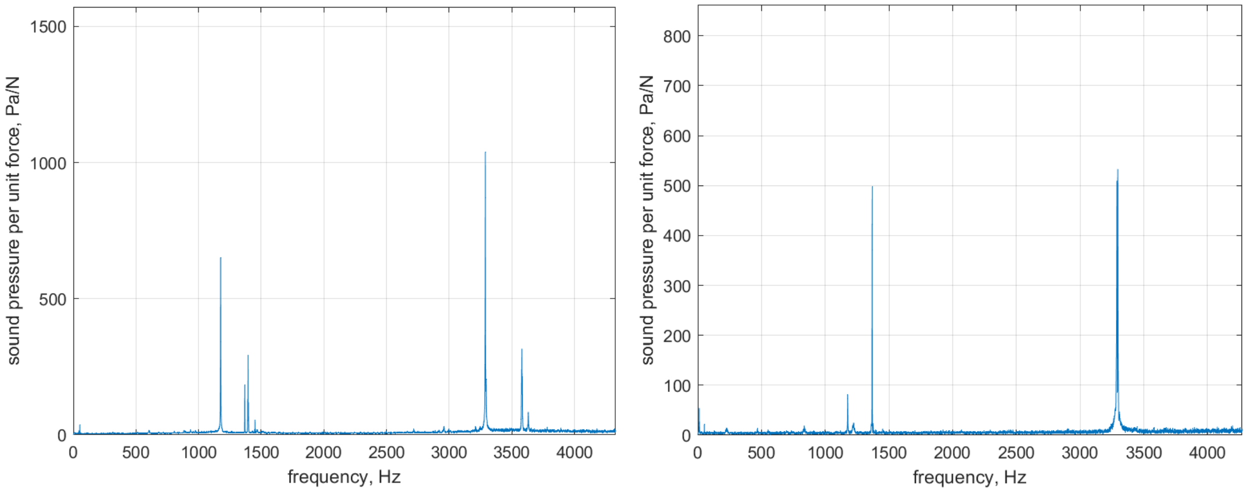

Figure 16. Average Sound Pressure Spectrum per force (Left: Low Tone Sound; Right: High Tone Sound)

As demonstrated in Figure 16, the average sound pressure spectrum under unit force indicates that the vibration intensity of the structural modes is significantly higher than expected in the frequency range of 3000-3500 Hz. This might be attributed to the ellipitical ring bell's relatively simple structure, which is easily excited by the striking locations, especially the second-order breathing mode. However, this issue is not insurmountable. Figure16 only reflects the dynamic characteristics of the elliptical ring; sound characteristics need to consider both dynamic characteristics and the spectrum of striking force. Since the striking force is not an instantaneous impulse, its spectrum is not linear. The excitation energy decreases with the increase in frequency. The rate of decline in input energy is affected by the material of the hammer. When the contact stiffness of the hammer is low, the force decays faster. Therefore, a hard plastic hammer was chosen and the experiment was repeated. It is worth noting that due to the inconsistency in the force of each strike, the data were normalized to make the fundamental frequency peaks of the two measurements the same.

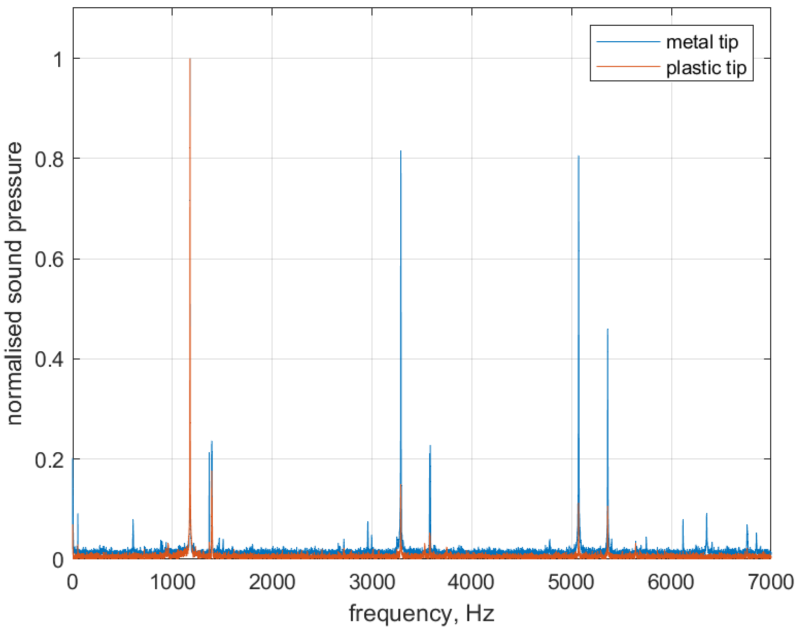

Figure 17. Normalised sound pressure spectrum when subject to different tips of hammer

Figure17 shows that the spectrum decays too fast with the hard plastic hammer, significantly reducing the high-frequency component of the elliptical ring. Although the expected pitch was heard, the timbre was thinner compared to the chime bell. Through literature [18], it was learned that the high-frequency component of the chime bell is crucial for the overall timbre. Hence, reducing the contact stiffness moderately, based on existing equipment, was considered. A simple method was proposed: applying a layer of transparent tape at the structural striking positions to reduce stiffness, as shown in Figure 18.

Figure 18. Application of the transparent type to tune the striking force

After this modification, the experiment was repeated, and the results are as shown in Figure 19.

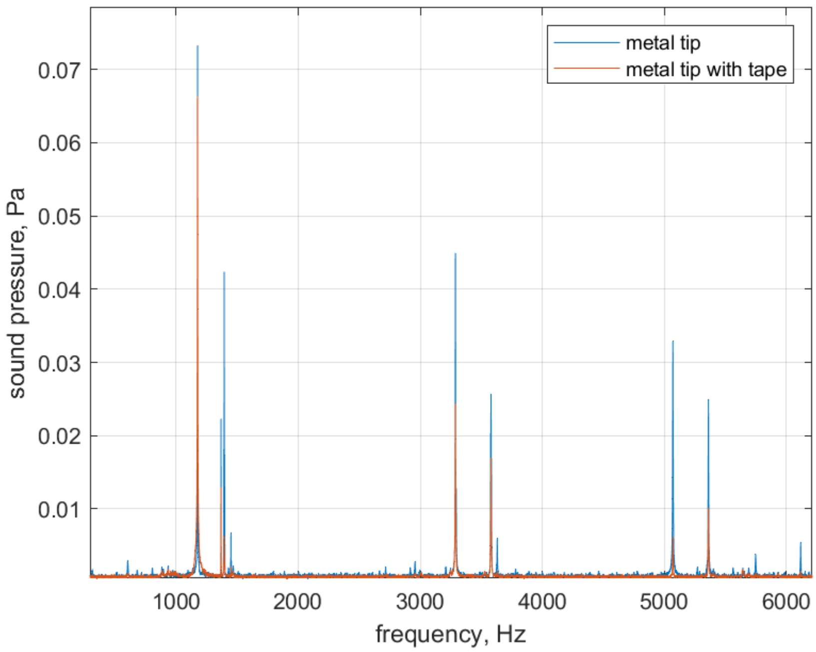

Figure 19. Normalized sound pressure spectrum when subject to different excitation configuration.

Figure 19 shows that the application of transparent tape makes the sound pressure spectrum peak at the fundamental frequency, while the amplitudes of other high-frequency sounds gradually decrease. Additionally, the secondary frequency peak is about 1/3 of the fundamental frequency peak. Subsequently, the spectra of the elliptical ring and the chime bell were compared. It’s worth noting that due to the inconsistency in the force of each strike, the data were normalized to make the fundamental frequency peaks of the two instruments the same.

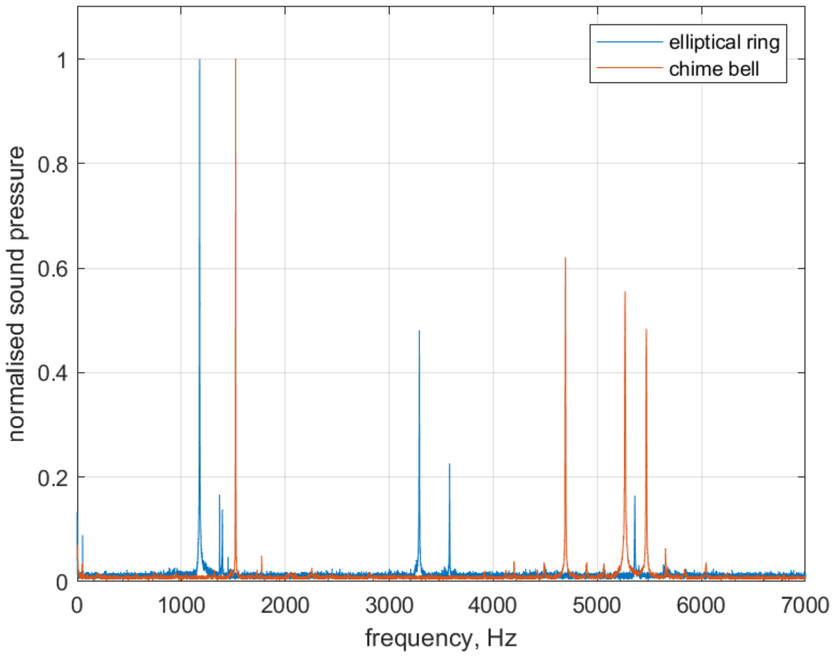

Figure 20. Normalised sound pressure spectrum: elliptical ring bell v.s. chime bell

According to the observations in Figure 20, a similar sound pressure ratio between high-frequency harmonics and the fundamental frequency is exhibited by the improved elliptical ring and the chime bell. From an auditory perspective, the timbre of the chime bell is extremely similar to that of the elliptical ring[19]. However, it was also noted that the fundamental frequency of the designed elliptical ring is not exactly the same as that of the chime bell, showing a difference of approximately 30%. This difference may stem from a mismatch between the material properties used in the finite element analysis and the actual manufacturing material.

The discrepancy between the calculated mass in the finite element model and the actual measured mass was first examined. For the cast iron elliptical ring model, the actual mass was 1664 grams, while the calculated mass in the model was 1743 grams, resulting in a difference of 4.7%. Since the mass is lower, it cannot account for the lower resonant frequency observed in the tests. Therefore, the more likely reason is the improper definition of the Young's modulus of the material. In the finite element analysis, standard steel material properties were used, but in reality, a cast iron process was used by the manufacturer, indicating that the actual material is likely cast iron. The Young's modulus of cast iron is generally much lower than that of ordinary steel, thus prompting further investigation of the impact of the Young's modulus using finite element analysis.

A new finite element analysis was conducted, where the material properties of the iron ring were changed to cast iron, and the physical properties of this material were displayed in Table 5.

Table 5. Material property of casted iron

Density	7200 kg/m3
Young’s modulus	150 MPa
Possion’s ratio	0.28

The results of the finite element modal analysis are shown in Figure 21. After accurately defining the material properties, two modes appeared at 1146 Hz and 1368 Hz, which are very close to the tonal frequencies obtained in the chime bell experiments, which were 1176 Hz and 1322 Hz, respectively. Although further optimization of the elliptical ring was not possible due to time constraints, the study successfully explored the design method of the elliptical ring and conducted thorough design work.

This section concentrated on studying the sound characteristics of the elliptical ring, which was optimized in the design. By selecting the final structural design and appropriate striking hammers, a sound resembling the timbre of the chime bell was successfully obtained. The final spectra of the positive strike and side strike are shown in Figure 21.

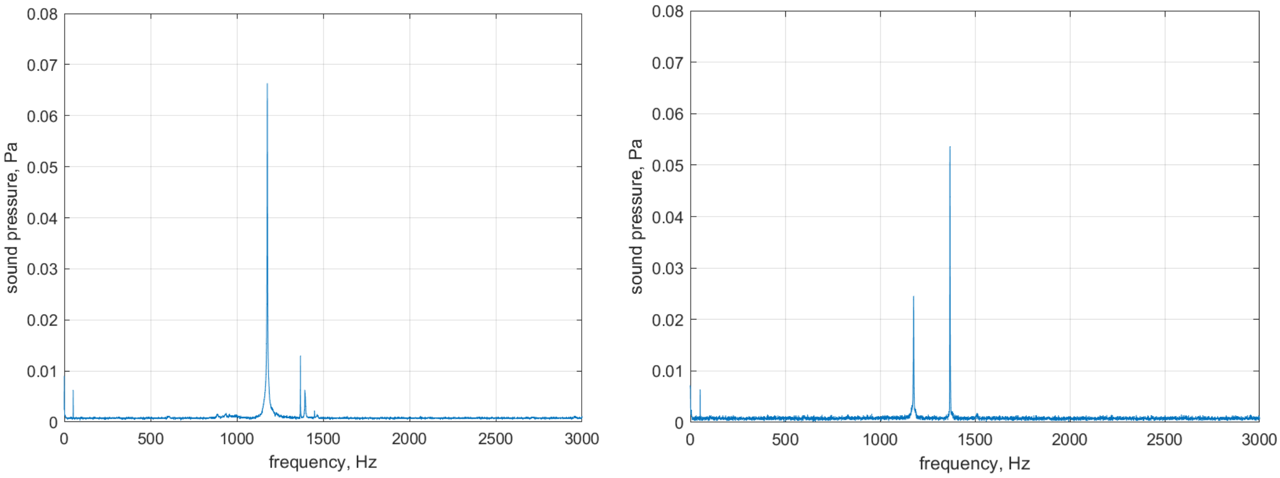

(a) (b)

Figure 21. Tonal frequency of elliptical ring (a) low frequency tone; (b) high frequency tone

7. Conclusion

The study embarked on exploring the sound generation mechanism of the chime bell, a unique musical instrument whose sound production is intricately tied to its combined tile structure. Striking various positions stimulates different structural vibrations, consequently producing sounds of differing pitches. Experiments indicated that modal excitation at the head drum and side drum positions could generate sounds around 1400Hz and 1750Hz, respectively.

A vibrational mode analysis, utilizing both finite elements and experimental approaches, was conducted to further understand the chime bell's sound generation mechanism. Results uncovered that distinct parts of the chime bell harbor different vibrational modes, integral to the sound component. Mode analysis facilitated the identification of modes corresponding to specific pitches of the chime bell.

In a bid to substantiate research conclusions, an attempt was made to simulate the chime bell sound utilizing a cast iron elliptical ring. This structure, a simplified model designed by the research team, emulates the sound production of the chime bell, reproducing the dual-tone effect of its sound. Although successful in simulating the chime bell's sound characteristics, some frequency deviation was noted through experimentation.

The research embraced design optimization methods to enhance the sound simulation model. Through multiple iterations, the elliptical ring's dimensions were adjusted to bring its vibrational modes more in line with those of the chime bell. The process implicated optimizing the geometric parameters of the elliptical ring to narrow the gap in sound frequency between it and the chime bell.

A subsequent study of the sound characteristics of the elliptical ring was undertaken. Validation through experimentation affirmed that the optimized elliptical ring could indeed reproduce the chime bell sound, albeit with a minor frequency deviation. This infers that sound reproduction and enhancement are achievable through design optimization.

Despite encountering certain limitations due to time constraints and limited resources, and acknowledging the presence of some frequency deviation in the sound produced by the cast iron elliptical ring model compared to the chime bell, future research might seek to further optimize the model. This could involve selectively stimulating specific modes while minimizing the response of other high-frequency modes by designing specific patterns and structures on the elliptical ring's surface to fine-tune frequency and modes.

In conclusion, this study immersed itself into unraveling the sound generation mechanisms and vibrational characteristics of the ancient Chinese chime bell and triumphed in reproducing its sound via design optimization using a cast iron elliptical ring model. Despite inherent challenges and limitations, this research bequeaths new insights and methodologies for the acoustical study of ancient chime bells. It highlights the pivotal role of the combined tile structure and vibrational modes, bestowing invaluable contributions to comprehending sound production mechanisms and vibrational characteristics in ancient chime bells. Furthermore, this research not only augments the preservation and propagation of chime bell culture but also amplifies our understanding of musical performance and acoustic science.

References

[1] Wang B T, Li B J, Huang P C, et al. A study of the acoustic properties of the Zenghouyi chimes [J]. Journal of Applied Acoustics and Vibration, 2022, 14 (1&2): 41 - 51.

[2] Han Baoqiang. On the acoustic factors in the formation process of bell rhythm [J]. Journal of Tianjin Conservatory of Music, 2006 (1): 25 - 30.

[3] PAN Duwu, LIU Guixing. Measurement of Sounding Frequency of Jinhou mu Chime [J]. Conservation of Cultural Relics and Archaeological Science, 2000, 12 (2): 5 - 8.

[4] JIA Longsheng, CHANG Binjiu, WANG Yuzhu, et al. Study on the vibration pattern of Zenghouyi chimes by laser holography [J]. Jianghan Archaeology, 1981 (1): 19 - 24.

[5] Zhang H, Yan Z Z, Yang C C, et al. Study on excitation of the two-tone acoustic characteristic of the chime bell of Marquis Yi of Zeng by finite element method [J]. Chinese Science Bulletin, 2007, 52 (16): 2167 - 2173.

[6] YAN Yanlai, KONG Lingda, CHAI Kangmin, et al. A study on the musical nature of the ancient Chinese chimes [J]. University Physics, 2004, 23 (2): 0 - 0.

[7] XU Guangmin, LIU Younian, SU Ge. Characteristics of sound shape and tuning method of copper bells with round mouth [J]. Special Casting and Nonferrous Alloys, 2007, 27 (9): 735 - 736.Zhang, Huai, et al. "Study on excitation of the two-tone acoustic characteristic of the chime bell of Marquis Yi of Zeng by finite element method." Chinese Science Bulletin 52.16 (2007): 2167 - 2173.

[8] Wu, Chih-Wei, Chih-Fang Huang, and Yi-Wen Liu. "Sound analysis and synthesis of Marquis Yi of Zeng's chime-bell set." Proceedings of Meetings on Acoustics. Vol. 19. No. 1. AIP Publishing, 2013.

[9] Shen, Sinyan. "Acoustics of ancient Chinese bells." Scientific American 256.4 (1987): 104 - 111.

[10] Han B Q. Test the efficiency of the two-tone bell. Musical Instrument (in Chinese), 2002, 7: 18 – 22.

[11] DeWoskin, Kenneth J. "Comment onThe bronze chime bells of the Marquis of Zeng: Babylonian biophysics in Ancient China'by EG McClain." (1987).

[12] Chung, Suk Choo, Chang Duck Kong, and Young Ha Yum. "A study on the dynamic characteristics of the Korean Yi-dynasty bell type structure." KSME Journal 1 (1987): 133 - 139.